Regulation of Fast-Spiking Basket Cell Synapses by the Chloride Channel ClC-2

Csaba Földy[1,2], Sang-Hun Lee[1], Robert J. Morgan[1] and Ivan Soltesz[1]

[1]Department of Anatomy and Neurobiology, University of California, Irvine

[2]Present address: Department of Molecular and Cellular Physiology, Stanford University, Palo Alto

Correspondence:

Csaba Földy, PhD

Department of Molecular and Cellular Physiology

Stanford University

Palo Alto, CA 94304-5552

Email: foldy@stanford.edu

Supplementary Fig. 1a: Recordings of PV-IPSCs and CCK-IPSCs with different intra-pipette [Cl^-]. (a_1) I-V plots with 4mM intra-pipette [Cl^-] (CsCl; PVBC: n=3 pairs, CCKBC: n=6 pairs; asterisks indicate $P<0.05$). Note that, under these recording conditions with close to physiological intracellular [Cl^-], the differences between the inward IPSCs were accompanied by differences in E_{GABAA} (inset; PVBC: –70.8±0.9 mV, n=8 pairs; CCKBC: –67.8±0.9 mV, n=13 pairs, P=0.04), indicating lower intracellular [Cl^-]$_i$ at PVBC synapses (note that the difference between E_{GABAA} values cannot be explained by intrinsic $GABA_A$ channel differences underlying the two types of IPSCs; note also that E_{GABAA} for CCKBC inputs was not changed in the presence of AM251: –68.3±0.7 mV, n=6 pairs). (a_2) I-V plots with higher intra-pipette [Cl^-] (40mM CsCl: PVBC: n=7 pairs; CCKBC: n=6 pairs; 120mM CsCl: PVBC: n=5 pairs, CCKBC: n=5 pairs; two-way ANOVA). Inset, middle: no difference in percentage of successfully evoked events (PVBC: n=6 pairs; CCKBC: n=6 pairs), indicating that the smaller amplitude of the inward PV-IPSCs is not due to voltage-dependency of the release probability. (a_3) Summary graph constructed from data in a_1&a_2 shows that the differences ($P<0.01$, one-way ANOVA with Tukey-Kramer multiple comparison test) between the amplitudes of inward PV-IPSCs and CCK-IPSCs are $[Cl^-]_{pip}$-dependent. Note that in these data sets, only the portion of the I-V curves from the CCK-IPSCs was considered that was unaffected by DSI. (a_4) The rectification of PV-IPSCs is also $[Cl^-]_{pip}$-dependent (control experiments showed that AM251 did not change the rectification of PV-IPSCs: 0.38±0.04, n=3 pairs, with 4mM [Cl^-]$_{pip}$). Note that similar results could also be obtained when an alternative measure of rectification of PV-IPSCs was used based on ratios of PV-IPSC amplitudes at voltages symmetrical around E_{GABAA}: 4mM $[Cl^-]_{pip}$: 0.64, measured ±20 mV from E_{GABAA}; 40 mM: 0.62, at ±40 mV from E_{GABAA}; 120 mM: 0.94, at ±40 mV from E_{GABAA} (note that the voltages were only approximately symmetrical around E_{GABAA}, because E_{GABAA} did not necessarily coincide with voltages at which data were obtained). Note also that there are two possible explanations for the Cl^- dependency in this data set, a hypothetical Cl^- regulating mechanism that is differentially active at the PVBC and CCKBC synapses, and/or a potential differential Cl^- sensitivity of the $GABA_A$ channels present at the two types of synapses. However, the differences between the E_{GABAA} values of the PV-IPSCs and CCK-IPSCs (inset in a_1) strongly favor the first possibility, i.e., differential regulation of intracellular [Cl^-] (note that the data shown in main Fig. 2d&e confirmed that the rectification of PV-IPSCs was not due to intrinsic $GABA_A$ receptor properties).

Supplementary Fig. 1b: Lack of marked outward rectification of PV-IPSCs in GCs of the dentate gyrus. Left panel: Lack of prominent hyperpolarization-gated, sustained Cl^--conductance in granule cells of the dentate gyrus (DG) in somatic recordings (compare with main left panel in Fig. 2a) (4mM: n_{soma}=6; 120mM: n_{soma}=5). Middle panel: I-V plot of PV-IPSCs in GCs (n=5 pairs). Right panel: Ratio of the

average ΔIPSC/ΔVs of the inward and outward portions of the I-V curves for dentate GCs. Note that the ratio of the average ΔIPSC/ΔVs of the PV-IPSCs is significantly larger in DG GCs compared to CA1 pyramidal cells (Pyr) (CA1 Pyr: 0.38±0.05, n=8 pairs; DG GC: 0.64±0.08, n=5 pairs, P=0.02). Note that the data in Supplementary Fig. 1b support a role for ClC–2 in the outward rectification of PV-IPSCs in CA1 pyramidal cells.

Supplementary Fig. 1c: Smaller amplitude of inward PV-IPSCs compared to CCK-IPSCs with K^+-based, Cs^+-free intra-pipette solution (solution #5 in the Suppl. Methods; PVBC: n=10 pairs; CCKBC: n=6 pairs). Inset: Differences in E_{GABAA} (PVBC: –73.1±0.7 mV, n=9 pairs; CCKBC: –70.8±0.9 mV, n=6 pairs, P=0.03). Note that these data indicate that the key observations of the main paper (i.e., the smaller inward PV-IPSCs and the differences in E_{GABAA}) can be also observed under conditions where KCC2 is active (note that the Cs^+-based intra-pipette solutions used in the rest of the study block KCC2, see Ref. 5 and references therein).

Supplementary Fig. 1d: Longer time to reversal of the inward (depolarizing) IPSCs to outward (hyperpolarizing) IPSCs in *ClC–2*$^{-/-}$ mice compared to *ClC–2*$^{+/+}$ after a brief period of intense presynaptic interneuronal activity evoked by extracellular stimulation. Left: Representative traces at –60 mV from *ClC–2*$^{-/-}$ and *ClC–2*$^{+/+}$ mice illustrate the longer time to reversal of the inward (depolarizing) IPSCs (marked with asterisks) following intense presynaptic interneuronal activity. Right: Summary data (*ClC–2*$^{+/+}$: n=8 cells; *ClC–2*$^{-/-}$: n=10 cells). Experimental details: Voltage clamp recordings were obtained from single CA1 pyramidal cells, with 4mM intra-pipette [Cl^-], solution #2 in the Suppl. Methods. Following baseline recordings at –60 mV during which outward IPSCs were evoked at 5 Hz (average amplitudes: *ClC–2*$^{+/+}$: 26.6±2.5 pA; *ClC–2*$^{-/-}$: 25.8±1.8 pA; P=0.78), the cells were depolarized to –20 mV for 4 sec and the stimulation frequency was increased to 50 Hz (for a total of 200 pulses) in order to simulate intense network activity-induced Cl^--loading of the cell; after the depolarizing step, the voltage was returned to –60 mV and the (now inward) IPSCs were again evoked at 5 Hz. Extracellular stimulation was evoked in the stratum pyramidale with a bipolar stimulating electrode, in the presence of ionotropic glutamate receptor blockers 10 µM DAP-5 and 5 µM NBQX, the $GABA_B$ receptor antagonist 2 µM CGP55845, and 10 µM AM251 to inhibit DSI. In order to simulate an approximately similar degree of synchronous activation of several presynaptic interneurons, stimulation intensity was adjusted to evoke IPSCs that were about 5 to 10 times larger than the average unitary IPSCs in paired recordings from PVBCs and pyramidal cells under similar conditions (at –60 mV with 4 mM intra-pipette [Cl^-], see Supplementary Fig. $1a_1$).

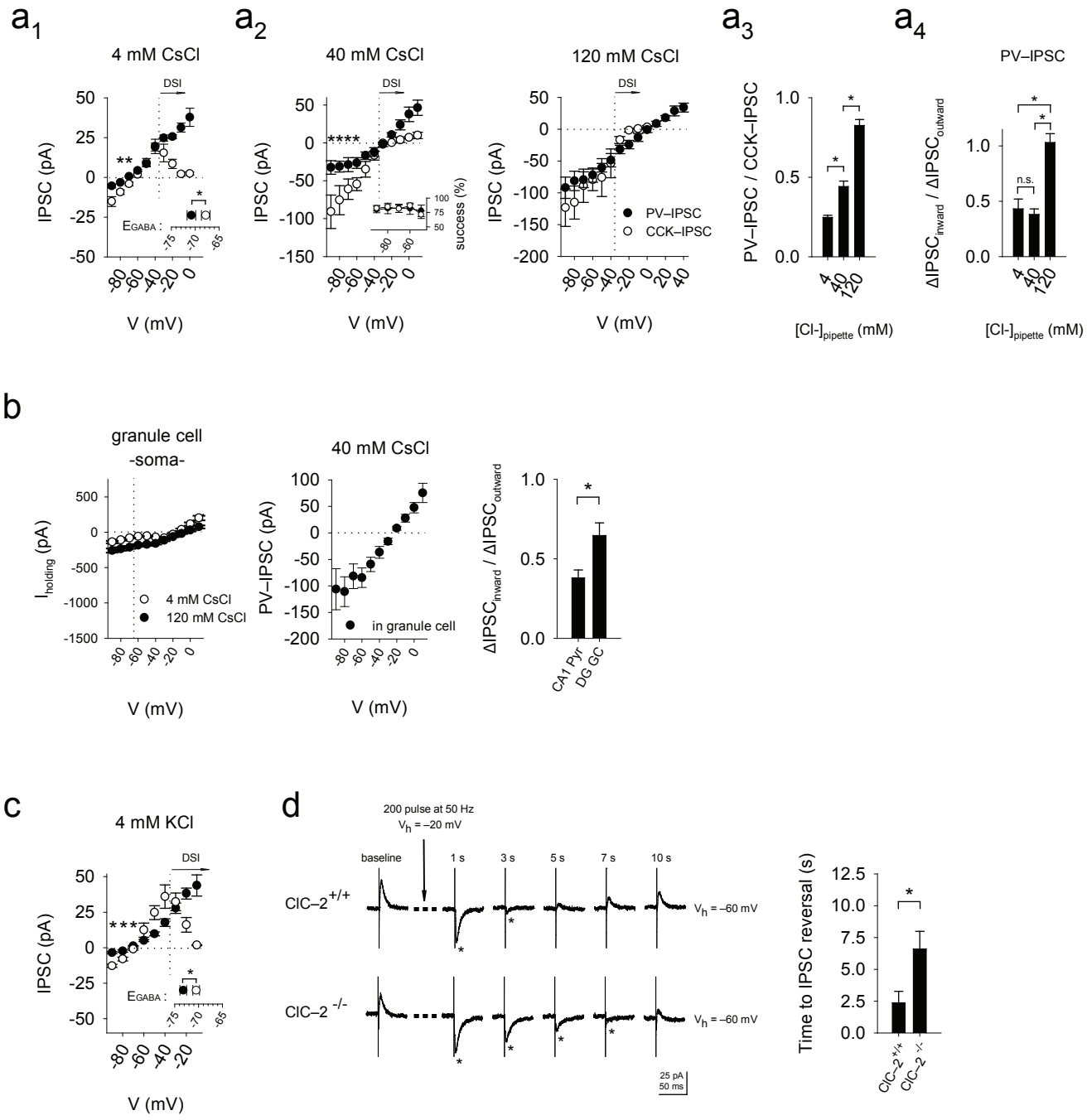
a1
4 mM CsCl
DSI
IPSC (pA)
EGABA
V (mV)
a2
40 mM CsCl
success (%)
a3
120 mM CsCl
PV–IPSC
CCK–IPSC
PV–IPSC / CCK–IPSC
[Cl-]pipette (mM)
a4
PV–IPSC
ΔIPSCinward / ΔIPSCoutward
n.s.
b
granule cell
-soma-
Iholding (pA)
4 mM CsCl
120 mM CsCl
in granule cell
CA1 Pyr
DG GC
c
4 mM KCl
d
200 pulse at 50 Hz
Vh = –20 mV
baseline
1 s
3 s
5 s
7 s
10 s
ClC–2+/+
ClC–2 -/-
Vh = –60 mV
25 pA
50 ms
Time to IPSC reversal (s)

Supplementary Methods

Electrophysiology Transverse hippocampal slices (350 μm) were prepared from 2–3 weeks old Sprague-Dawley rats or >3 weeks old mice. Slices were incubated in sucrose-containing artificial cerebrospinal fluid for an hour (ACSF; 85 mM NaCl, 75 mM sucrose, 2.5 mM KCl, 25 mM glucose, 1.25 mM NaH_2PO_4, 4 mM $MgCl_2$, 0.5 mM $CaCl_2$ and 24 mM $NaHCO_3$). Slices were visualized with an upright microscope (Olympus, BX-61WI) with infrared differential interference contrast (IR-DIC) optics. Whole-cell recording were obtained from the interneurons with patch-pipettes (3–5 MΩ) filled with internal solution containing 126 mM K-Gluconate, 4 mM KCl, 10 mM HEPES, 4 mM Mg-ATP, 0.3 mM Na-GTP, 10 mM Phosphocreatine and 0.2% biocytin (pH 7.2, 270–290 mOsm). All electrophysiological recordings were made at 33 °C. The interneurons were located in layer stratum radiatum and stratum pyramidale (see below). In paired recordings, the postsynaptic pyramidal cells (whole-cell voltage clamp configuration) were recorded with one of five internal solutions: 1) 40mM CsCl, 90mM K-Gluconate, 1.8 mM NaCl, 1.7 mM $MgCl_2$, 3.5 mM KCl, 0.05 mM EGTA, 10 mM Hepes, 2 mM Mg-ATP, 0.4 mM Na-GTP, 10 mM Phosphocreatine and 0.2% biocytin (pH 7.2, 270-290 mOsm); 2) 4mM CsCl, 126 Cs-Gluconate, 0.05 mM EGTA, 10 mM Hepes, 2 mM Mg-ATP, 0.4 mM Na-GTP, 10 mM Phosphocreatine and 0.2% biocytin; 3) 40mM CsCl, 90 Cs-Gluconate, 0.05 mM EGTA, 10 mM Hepes, 2 mM Mg-ATP, 0.4 mM Na-GTP, 10 mM Phosphocreatine and 0.2% biocytin; 4) 120 mM CsCl, 10 Cs-Gluconate, 0.05 mM EGTA, 10 mM Hepes, 2 mM Mg-ATP, 0.4 mM Na-GTP, 10 mM Phosphocreatine and 0.2% biocytin; 5) 126 mM K-Gluconate, 4 mM KCl, 10 mM HEPES, 4 mM Mg-ATP, 0.3 mM Na-GTP, 10 mM Phosphocreatine and 0.2% biocytin. Note that the majority of the recordings (with the exception of the data in Supplementary Fig. 1c) were obtained with a Cs^+-based intra-pipette solution which blocks KCC2 (Ref. 5). Recordings were made using MultiClamp700B amplifiers (Axon Instruments, Union City, CA). Signals were filtered at 4 kHz using a Bessel filter and digitized at 10 kHz with a Digidata 1440A analog–digital interface (Axon Instruments). Series resistances were carefully monitored, and the recordings were discarded if the series resistance changed significantly or reached 20 MΩ (for dendritic recordings, 35 MΩ). Current-voltage (I-V) plots (e.g., Fig. 1a) were constructed by evoking a series of unitary IPSCs in a systematic manner at holding potentials that were incrementally increased in steps of 10 mV, starting with –90 mV. The recorded traces were analyzed using the Clampfit 9.0 software (Axon Instruments). IPSCs were individually inspected and included in the analysis based on their onset latency following the presynaptic action potential (see Ref. 3 for details). For statistical analysis Student's t-test or ANOVA (with Tukey-Kramer multiple comparison test) was used, and the data are presented as mean ± s.e.m; significance was $P < 0.05$. For analysis of IPSC amplitudes (e.g., main Fig. 1a), the data sets

contained pairs with similar percentage of successfully evoked inward events (e.g., inset in the left panel of Supplementary Fig. $1a_2$).

Analysis of the I-V relationships The IPSC-membrane voltage (I-V) relationships were quantified by measuring the average change in IPSC amplitude for every 10 mV increase in holding potential ($\Delta IPSC/\Delta V$, in units of $pA \cdot 10^{-1} \cdot mV^{-1}$) reflecting the synaptic conductance for the inward and outward portions of the I-V curves. The measurement of the average $\Delta IPSC/\Delta V$ offers a simple, yet robust, approach for the quantification of the rectification present in the inward with respect to the outward currents. In this study, we chose not to use linear fits, or fits based on the Goldman-Hodgkin-Katz (GHK) formalism, for the following reasons. Linear fits were not used because they are not appropriate for curvilinear plots (such as the I-V curve of the PV-IPSCs in Fig. 1a). On the other hand, GHK formalism describes ion permeability through an idealized membrane only approximating ion fluxes through synaptic receptor-channels under biological conditions. For example, IPSCs are compound synaptic currents resulting from ion fluxes through multiple, spatially distributed synaptic contacts, and, clearly, the I-V curves of such IPSCs are influenced by known and unknown factors. A striking example of a known factor is provided by DSI itself in the case of the CCK-IPSCs, where the fitting with the GHK equation is clearly not appropriate when the entire voltage range is considered (i.e. from –90 to +10 mV, Fig1a). Because the confounding factor in the latter case is of known origin, the fitting of the data by GHK can be accomplished either within the hyperpolarized voltage range that is not affected DSI, or within the entire voltage range after application of a specific receptor blocker (inset in Fig1a). On the other hand, when an I-V curve is evidently influenced by a factor that is not known, as was the case for the PV-IPSCs, it is impossible to determine a priori a voltage range that is appropriate for the fitting with the GHK equation (identification of the latter confounding factor was the central motivation for the study).

Immunochemistry and neuroanatomy After recording, all slices were transferred into a fixative solution containing 4% paraformaldehyde and 0.2% picric acid in 0.1 M phosphate buffer. Slices were resectioned into 50 μm thin sections and immunoreactivity for cholecystokinin (CCK) was revealed with a mouse monoclonal antibody (mAb 9303, generously provided by the CURE Digestive Diseases Research Center, Antibody RIA Core, Los Angeles (NIH grant #DK41301); diluted 1:1000); immunoreactivity for parvalbumin (PV) was tested with a rabbit polyclonal antibody (PV-28; Swant, Bellinzona, Switzerland; diluted 1:1,000 in Tris-buffered saline containing 2% normal goat serum). The reactions were visualized with a goat anti-rabbit IgG conjugated to Alexa 488 (diluted 1:500 in Tris-buffered saline containing 2% normal goat serum; Molecular Probes) and a goat anti-mouse IgG conjugated to Alexa 594 (diluted 1:500), streptavidin conjugated to Alexa-350 for biocytin (diluted 1:500). The sections were then

mounted in Vectashield (Vector Laboratories) and analyzed with a fluorescent microscope. In order to reveal the presynaptic basket cell's axonal and dendritic arbors in detail, the biocytin-filled cells were subsequently visualized with 3,3'-diaminobenzidine tetrahydrochloride (0.015%) using a standard ABC kit (Vector). Identification of the interneurons: The identification of PVBCs or CCKBCs was done based on morphology and immunocytochemistry (Ref. 3). Briefly, based on the position and shape of the cell body in the inner stratum radiatum / pyramidale, the morphology of the dendrites visible in the IR-DIC, and the distinct electrophysiological "fingerprints" in spiking properties, it is possible to selectively record from these two basket cell populations with a high degree of confidence even before post-hoc identification. Importantly, all cells included in the paper were immunocytochemically identified as PV+ or CCK+. A large proportion of the axons were located within or adjacent to the pyramidal cell layer, i.e., the recorded cells were basket cells. In the paired recording experiments, the IPSC had fast rise-times and large amplitudes (see Ref. 3), in agreement with the anatomical and immunocytochemical data indicating that the recorded cells were basket cells. For counting of putative axon terminals for the experiments in Fig. 1c-d, the potential contact sites between the pair recorded and filled pre- and postsynaptic cells were closely examined under a 100x oil immersion objective, and the number of closely juxtaposed putative presynaptic terminals was counted on the soma or along the dendrites in 20 µm bins (Fig. 1d).